www.editada.org

International Journal of Combinatorial Optimization Problems and Informatics, 15(4), Nov 2024, 173-185. ISSN: 2007-1558. https://doi.org/10.61467/2007.1558.2024.v15i4.523

Kinematic analysis applied to a solar tracker driven by a 4-bar mechanism

Rafael A. Figueroa-Díaz[1], Josué R. Martínez-Mireles[2,], Francisco G. Urías[1], Rafael Moreno-Romero[1], Érica C. Ruiz-Ibarra[1], Javier De la Cruz-Soto[1], Jazmín Rodríguez-Flores[2]*
[1]Technological Institute of Sonora, Mexico.
[2] Polytechinc University of Pachuca (UPP), Mexico.

E-mails: *jmartinez@upp.edu.mx

Abstract. This paper presents the kinematic analysis of the eccentric crank-slider and crank-rocker mechanisms applied to control the 1-DOF in a solar tracker focused on improving the conversion of solar energy into electrical energy. The mechanisms for its construction and the kinematic equations that allow to know the state that keeps the movement in the working space of the tracker and its comparative analysis between them are presented. Finally, the construction to scale with 3D printing is shown to validate the functionality of each of the 4-bar systems.
Keywords: Solar tracker, crank-slider, crank-rocker, comparative analysis, 3D printing

Article Info
Received Sep 30, 2024
Accepted Oct 15, 2024

1 Introduction

Global warming has emerged as a significant issue in recent years (Abbass et al, 2022; Özcelík et al, 2016). Consequently, various technologies have been developed in the field of renewable energies, including the utilization of solar panels (Osman et al, 2023). An influential factor in optimizing energy conversion through this technology is solar radiation, so considering the panel's orientation in relation to the sun is crucial, as outlined in (Abbass et al, 2022). Mexico features regions with prolonged periods of high solar radiation which offer a natural geography conducive to harnessing this technology to its full potential. Located in the northern part of Mexico, the state of Sonora stands out as the region receiving the highest levels of solar radiation, averaging 5.6-5.8 kWh/(m^2/day), making it an ideal location for the establishment of solar power plants, as discussed in (Arancibia et al, 2014). The Numerical Weather Prediction (NWP) model was employed in (Sosa et al, 2018) in southern Sonora to assess solar radiation levels across different seasons. Likewise, a study conducted in (Sosa et al, 2019) explored a photovoltaic installation for the company Sales del Valle S. A. de C. V., aiming to achieve a 28% reduction in energy consumption through the deployment of panels mounted on a mechanical structure.

In solar panel technology, electrical energy conversion is predominantly contingent on the panel's orientation relative to the sun's rays and its temperature. In the 2013 study presented in (Anusha and Chandra, 2013), a comparative analysis between a fixed and a mobile panel demonstrated a 40% increase in electricity generation by manipulating one degree of freedom (DOF) of the panel. The study emphasized the electronic design of the tracking system, while the didactic panel was directly linked to the DC motor. Additionally, (Arreola et al, 2015) proposed the use of a 2-DOF tracker employing 24 VDC motors with a speed reducer coupled to the angular movement of the axles holding the panel. Orientation was determined using the algorithm proposed by (Walraven, 1977) as a reference, together with electronic instrumentation; this enabled maximizing power generation, which was subsequently compared with both a fixed system and the proposed system; the result was a 27.98% increase, with 0.3% of the total energy being consumed by the actuators. The study was conducted in the municipality of Texcoco, in the State of Mexico.

A comparative study of a 1-degree-of-freedom (1-DOF) and a 2-degree-of-freedom (2-DOF) solar tracker was presented in (Ray and Kumar, 2016). The first case involved the direct coupling of a DC motor to the shaft upon which the solar panel is installed, utilizing corresponding electronics for solar tracking. Subsequently, a second degree of freedom and its corresponding motor were applied to the same system to provide axle movement, complementing the electronic control system. Scale prototypes demonstrated that the 1-DOF system achieved 30% efficiency, while the 2-DOF system reached 40% efficiency when compared to a fixed panel at 21°.

In the same line of research, (Bhanu and Govindarajulu, 2022) presented a study on a 2-degree-of-freedom (2-DOF) tracker employing a worm screw to control panel orientation with direct coupling. DC motors were utilized to control the axle with spur gears. The electronic tracking system and a comparison of the tracker with a fixed panel were also discussed, revealing 30% efficiency when utilizing the proposed mobile system. The physically constructed systems were demonstrated at scale.

A similar proposal was outlined in (Nwanyanwu et al, 2017), where two DC actuators were applied to control both panel and axle movements with direct coupling between the shaft and the motor. The focus was on the system's electronic instrumentation; however, no evidence of the constructed prototype or field results were provided. In 2017, a 1-degree-of-freedom (1-DOF) tracker was introduced in (Hussan et al, 2017) that allowed controlling the axle, with the panel fixed at 35.47°. The system employed a DC motor coupled to a worm screw reducer connected to the shaft to facilitate the corresponding movement. The implementation of a solar panel parallel to the tracker was proposed, using a reflective surface to enhance electrical energy generation. The results were compared with those of a fixed panel, revealing that the proposed scheme allows for a 71.75% power efficiency compared to the fixed scheme. Like previous articles, the focus remains primarily on electronic instrumentation and the tracking algorithm. Meanwhile, (Özer et al, 2018) presented a comparative study between a fixed panel and a 2-degree-of-freedom (2-DOF) tracker, with the latter achieving 25% efficiency. The tracker utilizes a 100 W solar panel, and both panel and axle movements are individually controlled by a chain transmission system. The analysis presented in (Özer et al, 2018) concentrates on the development of electronic instrumentation for actuator tracking and control.

In 2019, (Ruelas et al, 2019) outlined the prototype for a 2-degree-of-freedom (2-DOF) tracker in which solar alignment is determined by an efficient orientation chart based on the presented electronic design. It employs a linear actuator for the angular control of the panel while proposing a 2-step bevel gear and worm screw system for the axle. The study, conducted in Obregon, Sonora, Mexico, demonstrated a 24% increase in electrical energy compared to a fixed system. The prototype was constructed at a 1:1 scale and incorporates four 250 W panels.

In (Mollahasanoglu and Okumus, 2021), servomotors with encoders were employed to drive both the panel and the axle of a 2-degree-of-freedom (2-DOF) tracker through a pair of spur gears. The authors detail the acquisition, processing, and control system for a 70 W panel reporting that building a 1:1 scale prototype resulted in a 24.7% efficiency improvement over a fixed system. Similarly, (Saad et al, 2023) introduced a prototype for a 2-DOF solar tracker utilizing linear actuators for panel and axle control. The 150 W panel was equipped with the corresponding electronic instrumentation, and the proposed system was compared with a fixed system, achieving a 25.19% increase in efficiency. In (Thungsuk et al, 2023), a cubic-shaped solar tracker featuring a 10 W panel installed on each edge of the cube was presented, with simultaneous axle movement on each panel facilitated by a chain transmission system. Additionally, the second degree of freedom for the angular movement of the panel utilizes the same transmission system coupled to a mechanism to generate the rocker output. The necessary electronic instrumentation and the system for detecting the position of the sun are presented, and the results were experimentally evaluated, considering cases such as a fixed panel with axle movement (1-DOF), a panel and axle movement (2-DOF), and a solar panel mounted on a structure. The results reveal that the 1-DOF tracker achieves an efficiency of 16.71% compared to the fixed system, while the 2-DOF tracker reaches 24.97%.

The abovementioned works provide a comprehensive approach to solar trackers, prioritizing both the electronic system and the sun position detection system. However, the design of the mechanical system for reducing the energy consumption required by the actuators is often overlooked. The research presented by (Long et al, 2014) focuses on the position development of a 2-DOF parallel manipulator coupled to a solar panel. The full-scale tracker was constructed to generate 400 W, and corresponding experimental tests were conducted, with solar position determined using the Local Condition Index (LCI) function. Meanwhile, the proposal in (Atencio et al, 2015) employs a 1-DOF tracker where an electric piston coupled to the shaft supporting the solar panel is controlled by a Proportional-Derivative (PD) scheme.

The tracker has also been constructed at a 1:1 scale. Intellectual property protection has been secured through the patent of the mechanical system that facilitates the tracker's movement, as detailed in (Stefano et al, 2012), where 3 planar mechanisms are employed to control the tracker's 2 degrees of freedom. Another patent, focusing on the mechanical system, is discussed in (Corio, 2013), which enables the control of 1-DOF in the solar panel tracker through a spur gear and worm screw system that can be integrated into the serial control of different solar panels. Meanwhile, (Thibert, 2018) implements a spherical tracker to control 2-DOF of the solar panel using 2 actuators.

In this study, the kinematic design of two 4-bar planar mechanisms is executed to control 1-DOF of a solar tracker. The corresponding comparison is presented to evaluate their applicability in solar panels. Finally, a practical-scale construction of

the proposed mechanisms is undertaken using additive manufacturing to validate the proposed equations and their functionality in the tracker.

2 Planar mechanisms for the control of one degree of freedom of solar tracker

2.1 Eccentric crank-rocker mechanism

Solar trackers facilitate the conversion of solar energy into electricity using solar panels, whose efficiency is contingent on their position relative to the sun. A prevalent contemporary approach involves installing the solar panels at a fixed orientation angle, as depicted in the following image.

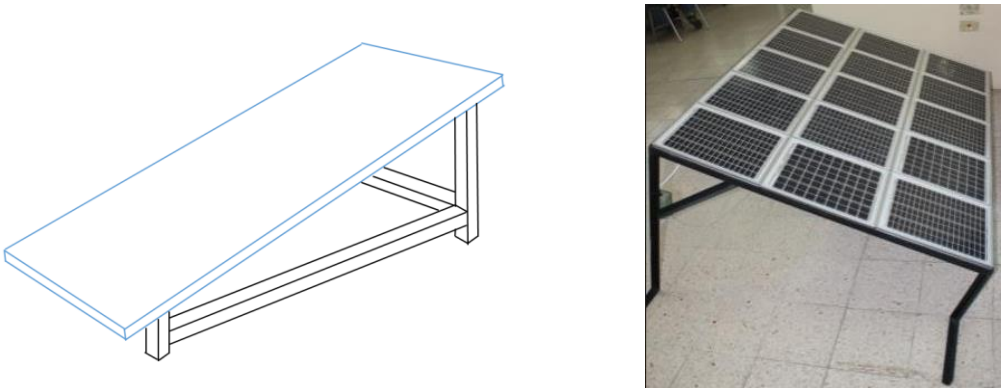

(**a**) (**b**)

Fig. 1. (**a**) Schematic diagram of solar panel on a structure. (**b**) Commercial Installation in a Housing Unit.

Figure 1 (a) and (b) depict a panel with a specific tilt, and for the southern region of Sonora, Mexico, a recommended fixed angle of approximately 27° can be applied, as suggested in (Sosa et al, 2019). Similarly, to enhance power generation, panel orientation towards the sun is essential, necessitating a system with at least two degrees of freedom, as illustrated in the following figure.

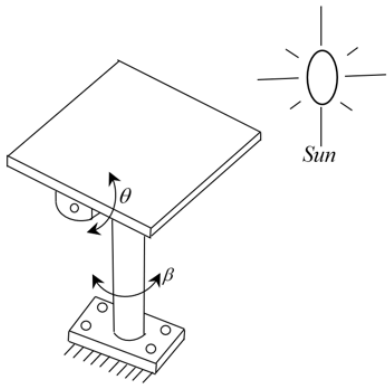

Fig. 2. Degrees of Freedom of the Solar Tracker.

In Figure 2, the two motions required to optimize the orientation of a solar tracker to solar position are depicted, where the angle β represents the axle movement and θ signifies the angular change of the solar panel. Various methods for controlling the required degrees of freedom are discussed in (Racharla and Rajan, 2017). Nevertheless, within the mechanical domain, purpose-specific mechanisms like 4-bar planar mechanisms can be utilized to control one degree of freedom in a solar tracker and integrate it into renewable energy systems.

This is a planar mechanism designed to generate a particular output pattern, consisting of 4 elements: ground, crank, coupler, and rocker arm. A common application of this element is in mechanical locking pliers, as shown in Figure 3 (a).

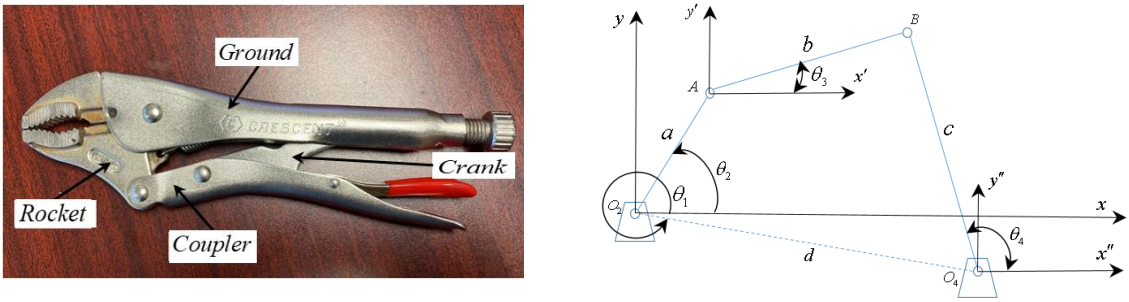

(**a**) (**b**)

Fig. 3. (**a**) Commercial 4-bar mechanism. (**b**) Schematic diagram of the off-center crank-rocker.

Figure 3 (a) depicts mechanical locking pliers, where the input force is applied to the coupler. For analysis, the eccentricity is assumed to be zero, and its mathematical solution, considering the crank as the input link, is detailed in (Norton, 2009; Myszka, 2009). However, a comprehensive solution for this application necessitates considering eccentricity in the mechanism, as illustrated in Fig. 3 (b). In this same figure, the lengths of the links are represented by the variables a, b, c, and d with the input force assumed to be located at link d, representing its crank. The output link corresponds to link c, the rocker arm. The corresponding vector diagram comprises a set of vectors in polar coordinates, as presented in Figure 4.

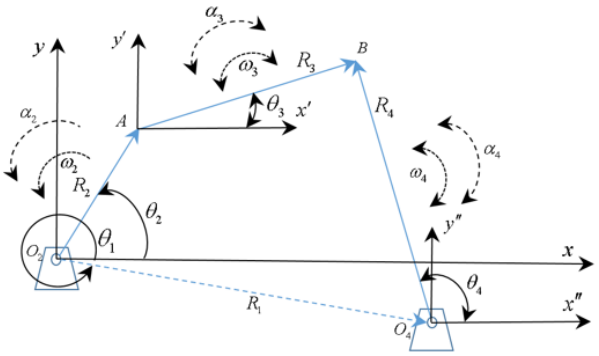

Fig. 4. Vector diagram of the off-center crank-rocker mechanism.

Note that in Figure 4, the angular value of the frame is non-zero ($\theta_1 \neq 0°$), generating an eccentricity in the mechanism and its general solution. Likewise, the links become vectors, originating in the fixed (x, y) and floating (x', y', x'', y''). coordinate systems. Therefore, the position equation given by the following expression is obtained from Figure 4:

$$a e^{i\theta_2} + b e^{i\theta_3} - c e^{i\theta_4} - d e^{i\theta_1} = 0 \tag{1}$$

Equation (1) represents the general vector position equation for the eccentric crank-rocker mechanism. The solution procedure using the complex method is detailed in (Norton, 2009), resulting in the position equations for the coupler and rocker, given below.

$$\theta_{3bal} = 2\tan^{-1}\left(\frac{-B-\sqrt{B^2-4AC}}{2A}\right) \tag{2}$$

and

$$\theta_{4bal} = \cos^{-1}\left(\frac{a\cos\theta_2 + b\cos\theta_3 - d\cos\theta_1}{c}\right) \tag{3}$$

where

$$A = -K_1\cos\theta_1 + K_2\cos(\theta_1 - \theta_2) + K_3 + \cos\theta_2$$
$$B = 2K_1 sen\theta_1 - 2sen\theta_2$$
$$C = K_1\cos\theta_1 + K_2\cos(\theta_1 - \theta_2) + K_3 - \cos\theta_2$$
$$K_1 = \frac{d}{a}$$
$$K_2 = \frac{d}{b}$$
$$K_3 = \frac{c^2 - a^2 - b^2 - d^2}{2ab}$$

Equations (2) and (3) represent the general solution for the off-center crank-rocker mechanism, constituting the general equations for this planar device, unlike the system presented in (Norton, 2009), which provides a specific solution. The velocity equations for the mechanism are expressed by the following expressions:

$$\omega_{3bal} = \frac{a\omega_2}{b}\frac{sen(\theta_4 - \theta_2)}{sen(\theta_3 - \theta_4)} \tag{4}$$

and

$$\omega_{4bal} = \frac{a\omega_2}{c}\frac{sen(\theta_2 - \theta_3)}{sen(\theta_4 - \theta_3)} \tag{5}$$

Likewise, the angular acceleration equations are given by the following expressions:

$$\alpha_{3bal} = \frac{C_1D_1 - A_1F_1}{A_1E_1 - B_1D_1} \tag{6}$$

and

$$\alpha_{4bal} = \frac{C_1E_1 - B_1F_1}{A_1E_1 - B_1D_1} \tag{7}$$

where:

$$A_1 = c\sin\theta_4$$
$$B_1 = b\sin\theta_3$$
$$C_1 = a\alpha_2\sin\theta_2 + a\omega_2^2\cos\theta_2 + b\omega_3^2\cos\theta_3 - c\omega_4^2\cos\theta_4$$
$$D_1 = c\cos\theta_4$$
$$E_1 = b\cos\theta_3$$
$$F_1 = a\alpha_2\cos\theta_2 - a\omega_2^2\sin\theta_2 - b\omega_3^2\sin\theta_3 + c\omega_4^2\sin\theta_4$$

where Equations (6) and (7) are considered fundamental for knowing the linear and torsional inertial forces.

2.2 Eccentric crank-slider mechanism

Another mechanism architecture is the crank-slider. A common application of this element can be found in a can crusher, as presented in Figure 5 (a) below.

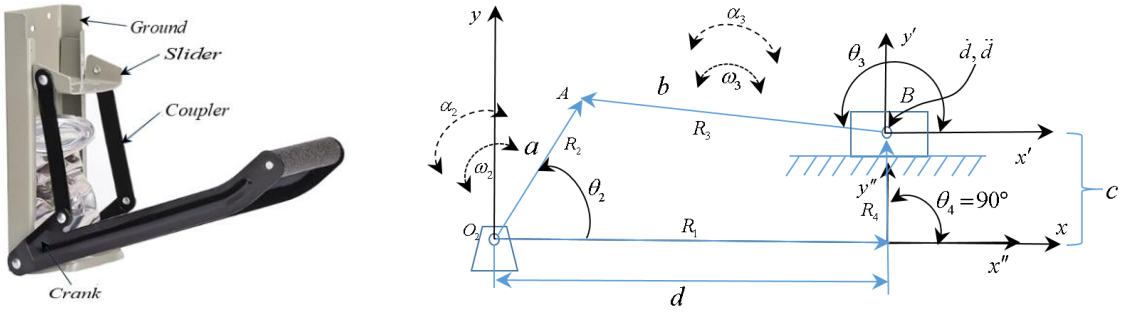

(**a**) (**b**)

Fig. 5. (a) Commercial can crusher mechanism. (**b**) Schematic diagram of off-center crank-slider.

The schematic diagram can be seen in Figure 5 (b). In this latter figure, the input link is the slider represented by node B. Therefore, the known variables are considered to be: a, b, c, d, while the variables to be determined are θ_2 and θ_3. The vector equation for crank-slider position is expressed in the following equation:

$$a e^{i\theta_2} - b e^{i\theta_3} - c e^{i\theta_4} - d e^{i\theta_1} = 0 \tag{8}$$

Using the methodology presented in (Norton, 2009), the position equations for the coupler link and the crank are given by the following mathematical expressions:

$$\theta_{2corr} = 2\tan^{-1}\left(\frac{-E \pm \sqrt{E^2 - 4DF}}{2D}\right) \tag{9}$$

and

$$\theta_{3corr} = 2\tan^{-1}\left(\frac{-H \pm \sqrt{H^2 - 4GI}}{2G}\right) \tag{10}$$

where:

$$D = K_4 + 2ad$$
$$E = -4ac$$
$$F = K_4 - 2ad$$
$$G = K_5 - 2bd$$
$$H = 4bc$$
$$I = K_5 + 2bd$$
$$K_4 = a^2 - b^2 + d^2 + c^2$$
$$K_5 = -a^2 + b^2 + c^2 + d^2$$

Equations (9) and (10) allow determining the angular position of the crank and coupler for any input value on the slider, whereas in (Norton, 2009) the input link for the crank-slider mechanism is the crank itself.

$$\omega_{2corr} = \frac{\dot{d}\cos\theta_3}{a\sin(\theta_3 - \theta_2)} \tag{1}$$

and

$$\omega_{3corr} = \frac{\dot{d}\cos\theta_2}{b\sin(\theta_3 - \theta_2)} \tag{12}$$

The velocity at any point of the crank and coupler, respectively, can be determined from Equations (11) and (12), while the mathematical expressions to ascertain the angular acceleration are the following:

$$\alpha_2 = \frac{-b\omega_3^2 + a\omega_2^2\cos(\theta_3 - \theta_2) + \ddot{d}\cos\theta_3}{a\sin(\theta_3 - \theta_2)} \tag{13}$$

and

$$\alpha_3 = \frac{a\omega_2^2 - b\omega_3^2\cos(\theta_3 - \theta_2) + \ddot{d}\cos\theta_2}{b\sin(\theta_3 - \theta_2)} \tag{14}$$

Equations (13) and (14) allow determining the angular acceleration of the crank and coupler, respectively, which, when combined with Equations (11) and (12), determine the linear accelerations with their angle of incidence — parameters used for the dynamic force analysis of the mechanism.

2.3 Eccentric crank-rocker mechanism

The proposed integration of the 4-bar mechanism with rocker arm output and kinematic motions governed by Equations (2) to (7) is shown in Figure 6.

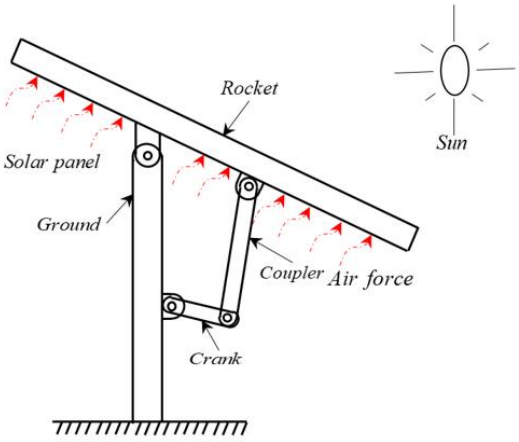

Fig 6. Integration of a crank-rocker into a solar tracker.

Figure 6 illustrates the proposed integration of the planar mechanism, where the coupling has been designed to control panel movement, optimizing its positioning relative to the sun. In this figure, the input actuator is assumed to be in the crank link (a), enabling control of the variable θ_2 . The rocker arm movement is coupled to the solar panel, and its position is determined by θ_4 . The kinematic design proposal is detailed in Figure. 7 (a) and (b).

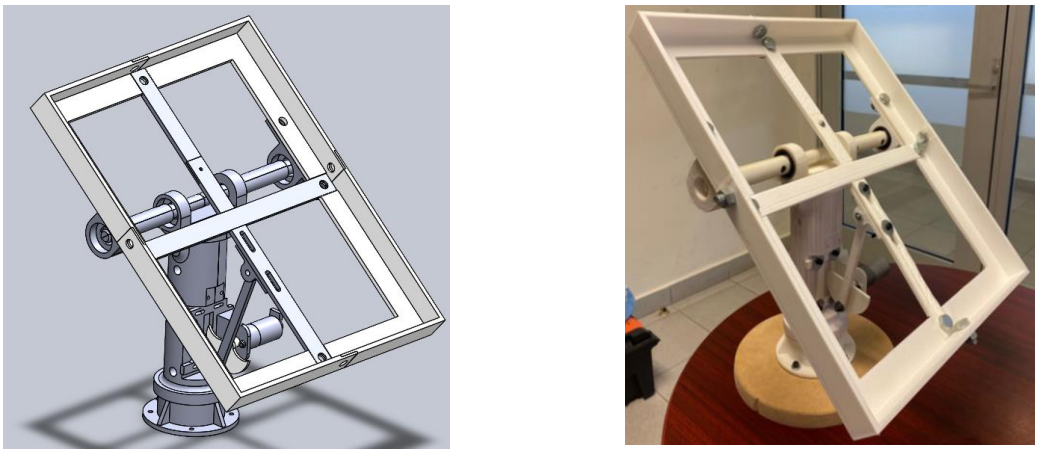

(**a**) (**b**)

Fig. 7. (a) Geometric design proposal made in CAD tool. (**b**) Functional 3-D printed model.

The figure above allows evaluating the functionality of the crank-slider mechanism in order to generate a desired output motion in the solar panel.

Adaptation of the crank-slider mechanism in the solar tracker for the second case study is shown in Figure 8.

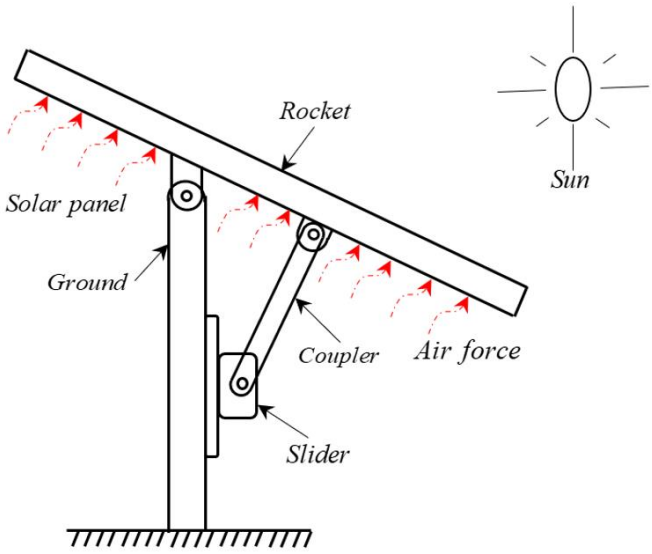

Fig. 8. Integration of a crank-slider into a solar tracker.

In Figure 8, it can be observed that the mechanism's sliding link represents the force and motion input into the system, while the crank establishes the coupling with the solar panel and represents the output variable of interest (θ_2). The kinematic design proposal is shown in Figure 9 (a) and (b).

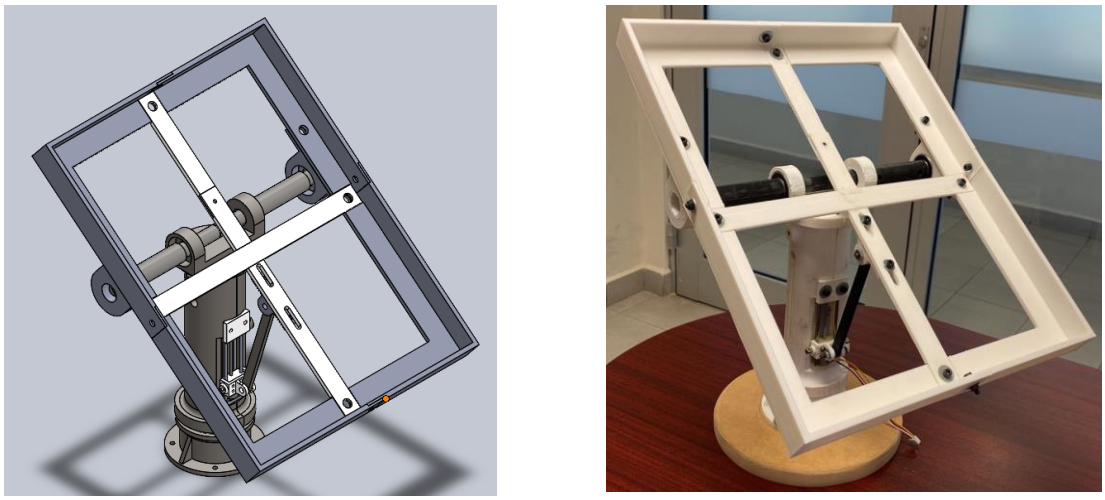

(**a**) (**b**)

Fig. 9. (a) Proposed geometric design of the crank-slider in CAD tool. (**b**) Functional 3D printed model of the crank-slider.

3 3. Results

3.1 Kinematic parameters of the crank-rocker

The rocker mechanism presented in Figure 7 was evaluated to determine its kinematic parameters using the elements presented in Table 1

Table 1. Numerical parameters for the scale crank-rocker mechanism.

Description	Variable	Value
Crank	a	$23 mm$
Coupler	b	$126 mm$
Rocker	c	$93.9 mm$
Ground	d	$155.46 mm$
Ground angle	θ_1	$342.8°$
Working Range	θ_2	$180-380°$
Input Angular Velocity	ω_2	$1.39 rpm$
Input Angular Acceleration	ω_2	$0 rad/seg^2$

The kinematic parameters of the output links — including position, velocity, and acceleration — can be determined by using the information from Table 1 in conjunction with Equations (2) to (7). However, for the current case study, particular attention is given to the panel's output motions relative to crank motion. The analysis of position and angular acceleration of the rocker arm generates the characteristic pattern depicted in Figure 10.

Figure 10 allows identifying that the minimum value of $\theta_{4Min}=94.47°$ when the crank is at $\theta_2=378.9°$, while the maximum position of the rocker arm is $\theta_{4Max}=122.83°$ for $\theta_2=198.7°$ making it possible to generate a $\Delta\theta=28.36°$. opening in the rocker arm, while the angular accelerations exhibit a minimum of $|\alpha_{4Min}|=0.0424 rad/seg^2$ when $\theta_2=187°$ and a maximum of $|\alpha_{4Max}|=0.0608 rad/seg^2$ for $\theta_2=373.4°$.

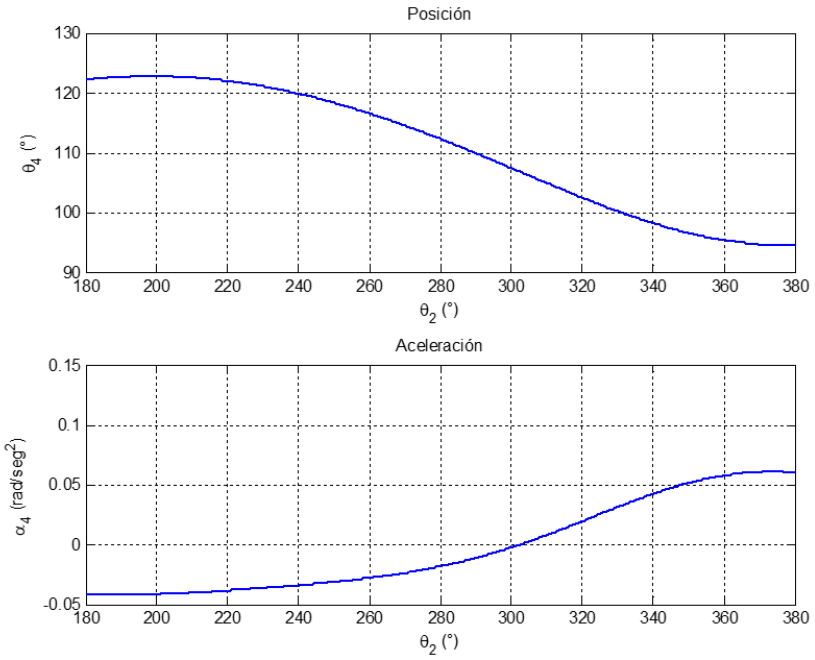

Fig. 10. Rocker arm position and acceleration pattern in its working range.

3.2 Kinematic parameters of the crank-slider

The kinematic parameters used in this mechanism maintain the same crank and coupler dimensions as presented in Table 1, while the values complementing the crank-slider are provided in Table 2.

Table 2. Numerical parameters for the scale crank-slider mechanism.

Description	Variable	Value
Eccentricity	c	$4.24\,mm$
Slider	d	$11-16\,mm$
Linear Slider Speed (manufacturer data)	$\dot{d}$	$3.33\,mm/seg$
Linear Slider Acceleration	$\ddot{d}$	$0\,mm/seg^2$

The kinematic parameters of the mechanism for the working range of the slider can be determined from the information in Table 1 and 2 and Equation. (9) to (14), as shown in Figure 11.

In the position and angular acceleration patterns presented in Figure 11, it is assumed that the system is in a stable state in which it is found that $\theta_{2Max}=91.20°$ when the slider is at $d=11mm$, while the minimum position is at $\theta_{2Min}=47.02°$ for an input of $d=16mm$. Similarly, $|\alpha_{2Max}|=0.0607\,rad/seg^2$ and $|\alpha_{2Min}|=0.4803\,rad/seg^2$ are obtained for the same slider positions, respectively.

Slider motion control is achieved by coupling a lead screw to a commercially available stepper motor, as shown in Figure 9 (b).

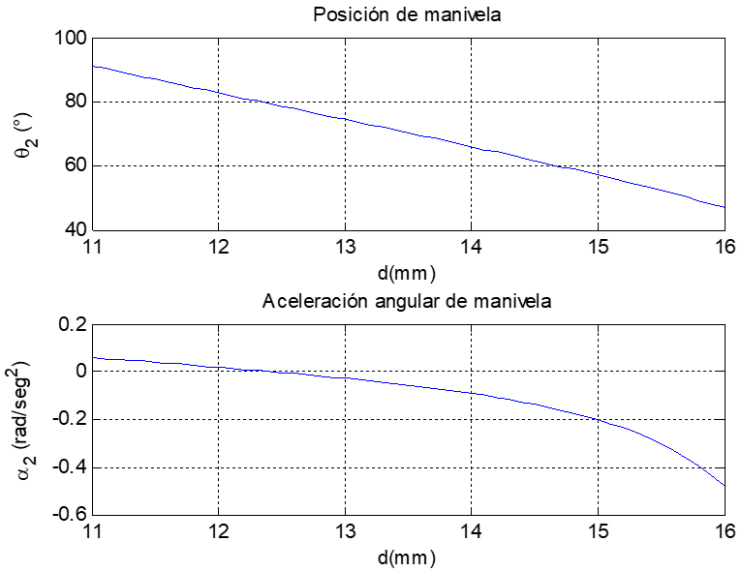

Fig. 11. Slider mechanism position and acceleration pattern in its working range.

4 Discussion

Solar trackers require at least 2-DOF to position the panel toward the sun for maximum power conversion. However, controlling each degree of freedom necessitates an actuator that consumes a portion of the generated electrical energy. Therefore, research is needed in different mechanical systems with the aim of reducing the required power. In the current research, crank-slider and crank-rocker mechanisms, as shown in Figures 7 and 9, were employed for the control of 1 degree of freedom, and their operation can be applied for this purpose. Kinematic equations (position, velocity, and acceleration) of the rocker mechanism were developed, considering eccentricity in the frame and input force located on the crank, resulting in Equations. (2) to (7), which constitute a general deduction compared to that presented in (Norton, 2009). For the crank-slider mechanism, the expressions for position, velocity, and acceleration are given by Equations. (9) to (14), considering that the slider is the link with the input motion. Patterns characteristic of position and angular acceleration were obtained based on Equations. (2) to (7) and considering a working range of $\theta_2 = 180 - 380°$, as shown in Figure 10. When compared with corresponding patterns for the crank-slider (see Figure 11), it is observed that the solar panel exhibits smoother motion in position and angular acceleration with the latter mechanism.

Considering the dynamic force analysis of the crank-slider and crank-rocker mechanisms, the inertial torque depends on angular acceleration and moment of inertia, which could be a crucial factor. It is essential to avoid abrupt acceleration changes that may damage the solar panel or the tracker components. During experimental tests of the constructed prototypes, the crank-rocker mechanism (see Figure 7 (b)), whose actuator consists of a DC motor and a gear reducer, required a constant power supply to sustain the panel in the desired position. In the case of the crank-slider (see Figure 9b)), the actuator is installed in the slider and comprises a DC motor directly coupled to a lead screw, allowing the solar panel to remain in the desired position even when deenergized.

5 Conclusions

Over the past few decades, the issue of global warming has gained worldwide relevance due to its negative impact on the planet. This has prompted the development of public policies supporting the reduction of greenhouse gases, and in the scientific realm, the emergence of the green energy sector. Among these, solar panels play a crucial role, but they require a specific position relative to the sun to maximize electrical energy conversion. Due to its geographical location, the state of Sonora is an exceptional place for solar energy capture, making it an attractive location for the establishment of solar parks in the region. This growth potential underscores the need to continue research and development in these systems.

One area of opportunity focuses on the mechanical system supporting the solar tracker. For the mechanical structure of the tracker, the use of the off-center crank-rocker and off-center crank-slider mechanisms is proposed to control one degree of freedom (1-DOF). The general kinematic equations for the off-center crank-rocker were developed considering that the input motion is in the crank link. Meanwhile, for the off-center crank-slider system, the corresponding kinematic equations were developed when the input motion was coupled to the slider.

Furthermore, the kinematic design and 3D construction of the scale model were carried out to test the position equations developed for the proposed mechanisms. Finally, through a comparative analysis in acceleration, it was concluded that the crank-slider mechanism exhibits smoother motion with respect to the rocker arm. It also has the advantage of holding the panel in position even when electrical power to the actuator is cut off. In contrast, the crank-rocker requires continuous power to keep the panel in place.

References

Abbass K, Zeeshan Q, Song H, Murshed M, Mahmood H, Younis I. (2022). A review of the global climate change impacts, adaptation and sustainable measures. Environmental Science and Pollution Research. 29. 42539-42559. https://doi.org/10.1007/s11356-022-19718-6.

Anusha K, Chandra M., (2013), Design and development of real time clock based efficient solar tracking system, International Journal of Engineering Research and Applications, 3(1), 1219-1223.

Arancibia B, Peón A, Riveros R, Quiñones J, Cabanillas R, Estrada C., (2014), Beam solar irradiation assessment for Sonora, México. Energy Procedia, 49, 2290-2296.

Arreola G, Quevedo N, Castro P, Bravo V, Reyes M., (2015), Design, construction and evaluation of a solar tracking system for a photovoltaic panel, Revista Mexicana de Ciencias Agrícolas, 6 (8), 1715-1727.

Atencio A, Gonzáles H, Muñoz Y., (2015), Diseño y construcción de un sistema de seguimiento solar de un eje para paneles fotovoltaicos, 13th LACCEI Annual International Conference: Engineering Education Facing the Grand Challenges, What Are We Doing?

Bhanu P, Govindarajulu K. (2022), Analysis and testing of dual axis solar tracker for standalone PV systems using worm gear, International Journal for Modern Trends in Science and Technology, 8(1), 1-8, https://doi.org/10.46501/IJMTST0801001.

Corio R. (2013), Single axis solar tracking system, US Patent. Patent Number. US 8,459,249 B2.

Hussan S, Muayyad N, Ozlim O., (2017), Efficient single axis sun tracker design for photovoltaic system applications, Journal of Applied Physics, 9 (2), 53-60, doi: 10.9790/4861-0902025360.

Long J, Han L, Hua C., (2014), Design and analysis of spacial parallel manipulator for dual axis solar tracking, Journal of the Chinese Society of Mechanical Engineers, 35(3), 221-231.

Mollahasanoglu M, Okumus H. (2021), Performance evaluation of the designed two-axis solar tracking system for Trabzon, IETE Journal of Research, DOI: 10.1080/03772063.2021.1973592.

Myszka D, (2012) “Máquinas y Mecanismos”. (4th ed.). Pearson.

Norton R. (2009). “Diseño de Maquinaria, síntesis y análisis de máquinas y mecanismos”. Mc. Graw Hill.

Nwanyanwu C, Dioha M, Sholanke O., (2017), Design, construction and test of solar tracking system using photo sensor, International Journal of Engineering Research & Technology. 6 (3).

Osman A, Chen L, Yang M, Msigwa M, Farghali M, Fawzy S, Rooney D, Yap P. (2023). Cost, environmental impact, and resilience of renewable under a changing climate: a review. Environmental Chemistry Letters, 21, 741-764, https://doi.org/10.1007/s10311-022-01532-8.

Özer T, Mustafa M, Oguz Y, Kivrak S, Sahin M., (2018), Double axis solar tracking system design and implementation, International Journal of Scientific & Engineering Research, 9(8).

Özcelík G, Ünver M, Temal C. (2016). Evaluation of the global warming impacts using a hybrid method based on fuzzy techniques: a case study in Turkey. Gazi University Journal of Science. 24 (4).

Racharla S, Rajan K., (2017), Solar tracking system – a review, International Journal of Sustainable Engineering, 10(2). https://doi.org/10.1080/19397038.2016.1267816.

Ray S, Kumar T. (2016), Design and development of tilted single axis and Azimuth-Altitude dual axis solar tracking systems, IEEE 1st International Conference on Power Electronics, Intelligent Control and Energy Systems (ICPEICES), Delhi, India, 1-6, doi: 10.1109/ICPEICES.2016.7853190.

Ruelas J, Muñoz F, Lucero B, Palomares J., (2019), PV tracking design methodology based on an orientation efficiency chart. Applied Sciences, 9 (5). https://doi.org/10.3390/app9050894.

Saad F, Attique J, Amjad A, Umer M, Ahmad M., (2023), Performance analysis of dual axis solar tracking system actuated through serial manipulators, International Conference on Emerging Trends in Electrical, Control, and Telecommunication Engineering (ETECTE), Lahore, Pakistan, 1-6.

Sosa T, Otero C, Peralta J, Miguez M, Rodríguez C. (2018) Sensitivity analysis of cumulus parameterizations for an irradiation simulation case. Sustainable Energy Technologies and Assessments, 28, 1-13.

Sosa T, Ambrosio L. (2019), Caso de estudio de cálculo y análisis de una instalación fotovoltaica para Sales del Valle S. A. de C. V., Revista La Sociedad Académica. , 53, 7-13.

Stefano M, Scarsella C, Batezzato A., (2012), Sun follower with parallel kinematics and process for controlling such follower. WIPO Patent. International publication number: WO 2012/131741 A1.

Thibert X. (2018), A spherical solar tracker, WIPO Patent. International publication number: WO 2018/178747 A1.

Thungsuk N, Tanaram T, Chaithanakulwat A, Savangboon T, (2023), Performance analysis of solar tracking systems by five-position angles with a single axis and dual axis, Energies,16.

Walraven R., (1977), Calculating the position of the sun, Solar Energy, 20 (5), 393-397. https://doi.org/10.1016/0038-092X(78)90155-X.